

## DCT TYPE-III FOR MULTICARRIER MODULATION

*M. Elena Domínguez-Jiménez, Gabriela Sansigre, Pedro Amo-López<sup>‡</sup>, and Fernando Cruz-Roldán<sup>‡</sup>*

Dpto. Matemática Aplicada  
ETSII, Universidad Politécnica de Madrid  
C. José Gutiérrez Abascal 2, 28006 Madrid, Spain  
phone: + (34) 913363104, fax: + (34) 913363018  
elena.dominguez@upm.es, gabriela.sansigre@upm.es

<sup>‡</sup> Dpto. Teoría de la Señal y Comunicaciones  
Escuela Politécnica Superior, Universidad de Alcalá  
28871 Alcalá de Henares, Madrid Spain  
phone: + (34) 918856693, fax: + (34) 918856699  
pedro.amo@uah.es, fernando.cruz@uah.es

### ABSTRACT

In this paper we propose the use of Discrete Cosine Transform Type-III (DCT3) for multicarrier modulation. There are two DCT3 (even and odd) and, for each of them, we derive the expressions for both prefix and suffix to be appended into each data symbol to be transmitted. Moreover, DCT3 are closely related to the corresponding inverse DCT Type-II even and odd. Furthermore, we give explicit expressions for the 1-tap per subcarrier equalizers that must be implemented at the receiver to perform the channel equalization in the frequency-domain. As a result, the proposed DCT3-based multicarrier modulator can be used as an alternative to DFT-based systems to perform Orthogonal Frequency-Division Multiplexing or Discrete Multitone Modulation.

### 1. INTRODUCTION

Multicarrier modulation (MCM) based on the discrete Fourier transform (DFT) has been adopted in many wired and wireless communication standards due to its ability to deal with severe multipath channel fading [1, 2, 3]. As DFT-based systems offer poor behaviour in noisy environments and they are very sensitive to carrier-frequency offsets (CFOs), among other problems, several researchers have been investigating the use of alternative discrete transforms for MCM (e.g., [4, 5, 6, 7]). In [4], it is shown how, by using the discrete cosine transform Type-II even (DCT2e -  $C_{2e}$ ), the symmetric channel matrix can be perfectly diagonalized without requiring channel knowledge at the transmitter. This is achieved by appending a symmetric prefix and a symmetric suffix to each symbol to be transmitted. In the above work, Al-Dhahir also shows that the DCT2e-based systems are more robust to frequency offsets than the DFT-based MCMs.

This work complements the results obtained in previous studies for DCT2e. The conditions to design DCT Type-III-based MCMs are derived, considering both DCT3 even and odd [8]. Fig. 1 shows the block diagram of the proposed system over a channel with additive noise. At the transmitter, an inverse DCT3 (even or odd) performs the multicarrier modulation. Then, the parallel/serial converter appends a prefix and a suffix into each block data symbol to be transmitted. The goal of the prefix and suffix is to obtain a channel matrix  $\mathbf{H}$  perfectly diagonalizable by the discrete cosine transform Type-III. Here, the prefix and also the suffix that must be appended into each data symbol to be

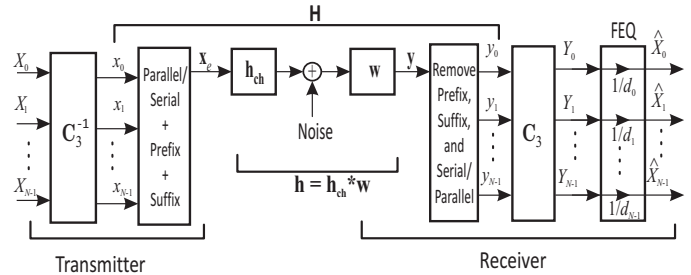


Figure 1: Block diagram of a DCT3-based multicarrier system over a channel with additive noise.

transmitted are obtained for both DCT3 even and odd. At the receiver, the first stage is a front-end prefilter  $w$  that forces the following symmetry in the global impulse response:  $\mathbf{h} = \mathbf{h}_{ch} * \mathbf{w} = (h_{-v}, \dots, h_{-1}, h_0, h_1, \dots, h_v)$ . Next, the serial/parallel converter removes both the prefix and the suffix before introducing each received data symbol in a block which performs the direct DCT3. Moreover, the channel equalization is carried out in the frequency-domain by a bank of scalars. With this purpose, the coefficients to perform the frequency-domain equalization under the zero-forcing criterion are also derived. Simulation results that show the performance comparison between the proposed system and OFDM, confirm superior performance of the former under carrier frequency offset (CFO) with or without the presence of a narrow-band interfering signal.

### 2. MATRIX REPRESENTATION OF THE CHANNEL

In Fig. 1, we consider a channel of impulse response  $\mathbf{h} = (h_{-v}, \dots, h_{-1}, h_0, h_1, \dots, h_v)$ . The transmission of an information symbol  $\mathbf{x}$  transforms it into the received symbol  $\mathbf{y}$  in the following way:

$$y_k = \sum_{m=-v}^v h_m x_{k-m} + z_k$$

where  $z_k$  is a term related to the additive noise.

In order to eliminate inter-block interference, we will add to the original symbol  $\mathbf{x}$  a left prefix  $\mathbf{x}_{pre}$  and a right suffix  $\mathbf{x}_{suf}$ , both of length  $v$ :

$$\mathbf{x}_e = \begin{bmatrix} \mathbf{x}_{pre} \\ \mathbf{x} \\ \mathbf{x}_{suf} \end{bmatrix}.$$

This work has been partially supported by the Universidad Politécnica de Madrid through the UPM TACA Research Group, and by Ministerio de Ciencia e Innovación (SPAIN) through the Research Project TEC2009-08133.

In matrix form, the receiving data symbol  $\mathbf{y}$  is given by

$$\mathbf{y} = \mathbf{H} \cdot \mathbf{x}_e + \mathbf{z},$$

where  $\mathbf{H}$  is the Toeplitz matrix of size  $N \times (N + 2v)$  defined as

$$\begin{bmatrix} h_v & \cdots & h_1 & h_0 & h_{-1} & \cdots & h_{-v} & 0 & \cdots & 0 \\ 0 & h_v & \ddots & h_1 & h_0 & \ddots & \ddots & h_{-v} & \ddots & \vdots \\ \vdots & \ddots & 0 \\ 0 & \cdots & 0 & h_v & \cdots & h_1 & h_0 & h_{-1} & \cdots & h_{-v} \end{bmatrix}.$$

It is easy to see that this matrix can be split as  $\mathbf{H} = [\mathbf{H}_{pre} \ \mathbf{H}_c \ \mathbf{H}_{suf}]$  where  $\mathbf{H}_{pre}$  contains its first  $v$  columns,  $\mathbf{H}_{suf}$  its last  $v$  columns, and  $\mathbf{H}_c$  the  $N$  remaining central ones:

$$\mathbf{H}_{pre} = \begin{bmatrix} h_v & \cdots & h_1 \\ 0 & \ddots & \vdots \\ \vdots & \ddots & h_v \\ 0 & \cdots & 0 \\ \vdots & & \vdots \\ 0 & \cdots & 0 \end{bmatrix}, \quad \mathbf{H}_{suf} = \begin{bmatrix} 0 & \cdots & 0 \\ \vdots & & \vdots \\ 0 & \cdots & 0 \\ h_{-v} & \cdots & 0 \\ \vdots & \ddots & \vdots \\ h_{-1} & \cdots & h_{-v} \end{bmatrix},$$

$$\mathbf{H}_c = \begin{bmatrix} h_0 & \cdots & h_{-v} & 0 & \cdots & 0 \\ \vdots & \ddots & \ddots & \ddots & \ddots & \vdots \\ h_v & & & & & 0 \\ 0 & & & & & h_{-v} \\ \vdots & \ddots & \ddots & & & \vdots \\ 0 & \cdots & 0 & h_v & \cdots & h_0 \end{bmatrix}. \quad (1)$$

Hence

$$\begin{aligned} \mathbf{H} \cdot \mathbf{x}_e &= [\mathbf{H}_{pre} \ \mathbf{H}_c \ \mathbf{H}_{suf}] \begin{bmatrix} \mathbf{x}_{pre} \\ \mathbf{x} \\ \mathbf{x}_{suf} \end{bmatrix} \\ &= \mathbf{H}_{pre} \cdot \mathbf{x}_{pre} + \mathbf{H}_c \cdot \mathbf{x} + \mathbf{H}_{suf} \cdot \mathbf{x}_{suf}, \end{aligned}$$

so the components of the block symbol are transformed by  $\mathbf{H}_c$ , whereas the appended left prefix is multiplied by  $\mathbf{H}_{pre}$ , and the appended right suffix is multiplied by  $\mathbf{H}_{suf}$ .

Let us suppose that the prefix and suffix are obtained linearly from  $\mathbf{x}$ , say

$$\begin{aligned} \mathbf{x}_{pre} &= \mathbf{G}_{pre} \cdot \mathbf{x}, \\ \mathbf{x}_{suf} &= \mathbf{G}_{suf} \cdot \mathbf{x}, \end{aligned}$$

where  $\mathbf{G}_{pre}, \mathbf{G}_{suf}$  are the left and right extension matrices. The whole transformation is given as

$$\begin{aligned} \mathbf{y} &= (\mathbf{H}_{pre} \cdot \mathbf{G}_{pre} + \mathbf{H}_c + \mathbf{H}_{suf} \cdot \mathbf{G}_{suf}) \cdot \mathbf{x} + \mathbf{z} \\ &= \mathbf{H}_{equiv} \cdot \mathbf{x} + \mathbf{z}. \end{aligned}$$

Notice that

$$\begin{aligned} \mathbf{H}_{pre} \cdot \mathbf{G}_{pre} &= \begin{bmatrix} h_v & \cdots & h_1 \\ 0 & \ddots & \vdots \\ \vdots & \ddots & h_v \\ 0 & \cdots & 0 \\ \vdots & & \vdots \\ 0 & \cdots & 0 \end{bmatrix} \mathbf{G}_{pre} = \\ &= \begin{bmatrix} \begin{bmatrix} h_v & \cdots & h_1 \\ 0 & \ddots & \vdots \\ \vdots & \ddots & h_v \end{bmatrix} \mathbf{G}_{pre} \\ \mathbf{O} \end{bmatrix} \end{aligned} \quad (2)$$

$$\begin{aligned} \mathbf{H}_{suf} \cdot \mathbf{G}_{suf} &= \begin{bmatrix} 0 & \cdots & 0 \\ \vdots & & \vdots \\ 0 & \cdots & 0 \\ h_{-v} & \cdots & 0 \\ \vdots & \ddots & \vdots \\ h_{-1} & \cdots & h_{-v} \end{bmatrix} \mathbf{G}_{suf} = \\ &= \begin{bmatrix} \mathbf{O} \\ \begin{bmatrix} h_{-v} & \cdots & 0 \\ \vdots & \ddots & \vdots \\ h_{-1} & \cdots & h_{-v} \end{bmatrix} \mathbf{G}_{suf} \end{bmatrix}, \end{aligned} \quad (3)$$

where  $\mathbf{O}$  is the null matrix. These expressions will help us to follow the development of the next sections.

### 3. DISCRETE COSINE TRANSFORM TYPE-III

#### 3.1 DCT3 even

The  $N$ -length DCT3 even (DCT3e) is given by the matrix  $\mathbf{C}_{3e}$  whose entries are (following [9]),

$$(\mathbf{C}_{3e})_{k,j} = 2a_j \cos\left(\frac{(2k+1)j\pi}{2N}\right), \quad k, j = 0, \dots, N-1,$$

where

$$a_j = \begin{cases} \frac{1}{2}, & \text{if } j = 0, \\ 1, & \text{otherwise.} \end{cases} \quad (4)$$

Let us recall that  $\mathbf{C}_{3e}$  is not orthogonal, but it is related to the orthogonal DCT2 even matrix  $\mathbf{C}_{2e}$ , which is defined in [4] as

$$(\mathbf{C}_{2e})_{k,j} = \sqrt{\frac{2}{N}} b_k \cos\left(\frac{k(2j+1)\pi}{2N}\right) \quad k, j = 0, \dots, N-1$$

being

$$b_k = \begin{cases} \frac{1}{\sqrt{2}}, & \text{if } k = 0, \\ 1, & \text{otherwise.} \end{cases}$$

In fact, the inverse of  $\mathbf{C}_{3e}$  is  $\mathbf{C}_{2e}$  up to a multiplicative factor in each row:

$$\mathbf{C}_{3e}^{-1} = \text{diag}\left(\sqrt{2}, 1, \dots, 1\right) \frac{\mathbf{C}_{2e}}{\sqrt{2N}}.$$

This means that the inverse DCT3 can be implemented as a DCT2 followed by the 1-tap per subcarrier equalizer  $\frac{1}{\sqrt{N}}, \frac{1}{\sqrt{2N}}, \dots, \frac{1}{\sqrt{2N}}$ . Conversely, as

$$\mathbf{C}_{3e} = \mathbf{C}_{2e}^{-1} \text{diag}(\sqrt{N}, \sqrt{2N}, \dots, \sqrt{2N}),$$

the DCT3 can be performed as an equalizer followed by an inverse DCT2. With this in mind, following [8], for the matrix  $\mathbf{H}_{equiv}$  to be diagonalized via  $\mathbf{C}_{3e}$ , it needs to be written as  $\mathbf{H}_{equiv} = \mathbf{T} + \mathbf{M}_{3e}$ , where  $\mathbf{T}$  is the Toeplitz matrix of order  $N$

$$\mathbf{T} = \begin{bmatrix} t_0 & t_1 & \cdots & t_{N-2} & t_{N-1} \\ t_1 & \ddots & \ddots & \ddots & t_{N-2} \\ \vdots & & & & \vdots \\ t_{N-2} & \ddots & \ddots & \ddots & t_1 \\ t_{N-1} & t_{N-2} & \cdots & t_1 & t_0 \end{bmatrix}, \quad (5)$$

and  $\mathbf{M}_{3e}$  is a matrix of the kind

$$\mathbf{M}_{3e} = \begin{bmatrix} 0 & t_1 & t_2 & \cdots & \cdots & t_{N-2} & t_{N-1} \\ 0 & t_2 & t_3 & & & t_{N-1} & 0 \\ 0 & t_3 & & & & 0 & -t_{N-1} \\ \vdots & & & & 0 & -t_{N-1} & \\ \vdots & & & & & \vdots & \vdots \\ \vdots & & t_{N-1} & & & \vdots & \vdots \\ \vdots & t_{N-1} & 0 & & & -t_3 & \\ 0 & 0 & -t_{N-1} & \cdots & & -t_3 & -t_2 \end{bmatrix}.$$

Note that  $\mathbf{M}_{3e}$  is not a Hankel matrix, but it comes from a Hankel matrix whose first column has been set to zero. We need to guarantee

$$\mathbf{H}_c + \mathbf{H}_{pre} \cdot \mathbf{G}_{pre} + \mathbf{H}_{suf} \cdot \mathbf{G}_{suf} = \mathbf{T} + \mathbf{M}_{3e}.$$

As  $\mathbf{H}_c$  of Equation (1) is a Toeplitz matrix, we can set  $\mathbf{T} = \mathbf{H}_c$ , and it suffices to build  $\mathbf{G}_{pre}$  and  $\mathbf{G}_{suf}$  so that  $\mathbf{H}_{pre} \cdot \mathbf{G}_{pre} + \mathbf{H}_{suf} \cdot \mathbf{G}_{suf}$  equals

$$\mathbf{M}_{3e} = \begin{bmatrix} 0 & h_1 & \cdots & h_v & 0 & \cdots & 0 \\ \vdots & \vdots & & & & & \vdots \\ 0 & h_v & & & & & 0 \\ 0 & 0 & & & & & -h_v \\ \vdots & \vdots & & & & & \vdots \\ 0 & 0 & \cdots & 0 & -h_v & \cdots & -h_2 \end{bmatrix}.$$

By means of Equations (2) and (3) we obtain that

$$\mathbf{H}_{pre} \mathbf{G}_{pre} + \mathbf{H}_{suf} \mathbf{G}_{suf} = \mathbf{M}_{3e}$$

if and only if

$$\begin{bmatrix} h_v & \cdots & h_1 \\ 0 & \ddots & \vdots \\ \vdots & \ddots & h_v \end{bmatrix} \mathbf{G}_{pre} = \begin{bmatrix} 0 & h_1 & \cdots & h_v & 0 & \cdots & 0 \\ \vdots & \vdots & & & & & \vdots \\ 0 & h_v & & & & & 0 \end{bmatrix},$$

$$\begin{bmatrix} h_v & \cdots & 0 \\ \vdots & \ddots & \vdots \\ h_1 & \cdots & h_v \end{bmatrix} \mathbf{G}_{suf} = \begin{bmatrix} 0 & 0 & \cdots & \cdots & 0 \\ 0 & & & & -h_v \\ \vdots & & & & \vdots \\ 0 & \cdots & -h_v & \cdots & -h_2 \end{bmatrix}.$$

Thus, the unique solution is

$$\mathbf{G}_{pre} = \begin{bmatrix} \mathbf{O}_{v \times 1} & \mathbf{J}_v & \mathbf{O}_{v \times (N-1-v)} \\ \mathbf{O}_{v \times (N+1-v)} & \mathbf{O}_{1 \times (v-1)} \\ & & -\mathbf{J}_{v-1} \end{bmatrix},$$

$$\mathbf{G}_{suf} = \begin{bmatrix} \mathbf{O}_{v \times (N+1-v)} & \mathbf{O}_{1 \times (v-1)} \\ & -\mathbf{J}_{v-1} \end{bmatrix},$$

where  $\mathbf{J}_n$  denotes the antidiagonal permutation matrix of order  $n$ . Hence, the prefix and the suffix are

$$\mathbf{x}_{pre} = \mathbf{G}_{pre} \cdot \mathbf{x} = [x_v \ x_{v-1} \ \cdots \ x_1]^T,$$

$$\mathbf{x}_{suf} = \mathbf{G}_{suf} \cdot \mathbf{x} = [0 \ -x_{N-1} \ \cdots \ -x_{N-v+1}]^T.$$

In summary, we have to apply a whole-point symmetry on the left and a whole-point antisymmetry on the right of the original symbol. With this prefix and suffix, the channel matrix  $\mathbf{H}_{equiv}$  turns out to be perfectly diagonalized by the DCT3 even.

### 3.2 DCT3 odd

In this subsection, we discuss the same problem as in the previous one but for the DCT3 odd (DCT3o) given by the matrix  $\mathbf{C}_{3o}$  of [9]:

$$(\mathbf{C}_{3o})_{k,j} = 2a_j \cos\left(\frac{(2k+1)j\pi}{2N-1}\right), \quad k, j = 0, \dots, N-1,$$

where  $a_j$  is defined in Equation (4).

It is not orthogonal but the inverse of this DCT3 odd may also be computed by means of a DCT2 odd followed by an eventual 1-tap per subcarrier equalizer.

By using the results given in [8], for the matrix  $\mathbf{H}_{equiv}$  to be diagonalized via  $\mathbf{C}_{3o}$ , it needs to have the form  $\mathbf{H}_{equiv} = \mathbf{T} + \mathbf{M}_{3o}$  where  $\mathbf{T}$  is the Toeplitz matrix of order  $N$  defined in (5) and

$$\mathbf{M}_{3o} = \begin{bmatrix} 0 & t_1 & t_2 & \cdots & \cdots & t_{N-1} \\ 0 & t_2 & t_3 & & & t_{N-1} & -t_{N-1} \\ 0 & t_3 & & & & -t_{N-1} & -t_{N-2} \\ \vdots & & & & & \vdots & \vdots \\ \vdots & & & & & \vdots & \vdots \\ 0 & -t_{N-1} & -t_{N-2} & \cdots & & -t_2 & -t_1 \end{bmatrix}.$$

Note that  $\mathbf{M}_{3o}$  also comes from a Hankel matrix whose first column has been set to zero. We have to build the matrices  $\mathbf{G}_{pre}$  and  $\mathbf{G}_{suf}$  so that  $\mathbf{H}_{pre} \mathbf{G}_{pre} + \mathbf{H}_{suf} \mathbf{G}_{suf}$  equals

$$\mathbf{M}_{3o} = \begin{bmatrix} 0 & h_1 & \cdots & h_v & 0 & \cdots & 0 \\ \vdots & \vdots & & & & & \vdots \\ 0 & h_v & & & & & 0 \\ 0 & 0 & & & & & -h_v \\ \vdots & \vdots & & & & & \vdots \\ 0 & 0 & \cdots & 0 & -h_v & \cdots & -h_1 \end{bmatrix}.$$

In this case, we obtain that this is possible if and only if

$$\begin{bmatrix} h_v & \cdots & h_1 \\ 0 & \ddots & \vdots \\ \vdots & \ddots & h_v \end{bmatrix} \mathbf{G}_{pre} = \begin{bmatrix} 0 & h_1 & \cdots & h_v & 0 & \cdots & 0 \\ \vdots & \vdots & & & & & \vdots \\ 0 & h_v & & & & & 0 \end{bmatrix},$$

$$= \begin{bmatrix} 0 & h_1 & \cdots & h_v & 0 & \cdots & 0 \\ \vdots & \vdots & & & & & \vdots \\ 0 & h_v & & & & & 0 \end{bmatrix},$$

$$\begin{aligned} & \begin{bmatrix} h_v & \cdots & 0 \\ \vdots & \ddots & \vdots \\ h_1 & \cdots & h_v \end{bmatrix} \mathbf{G}_{suf} = \\ & = \begin{bmatrix} 0 & 0 & & & -h_v \\ \vdots & \vdots & & & \vdots \\ 0 & 0 & \cdots & 0 & -h_v & \cdots & -h_1 \end{bmatrix}. \end{aligned}$$

Thus, the unique solution is

$$\begin{aligned} \mathbf{G}_{pre} &= \begin{bmatrix} \mathbf{O}_{v \times 1} & \mathbf{J}_v & \mathbf{O}_{v \times (N-1-v)} \end{bmatrix}, \\ \mathbf{G}_{suf} &= \begin{bmatrix} \mathbf{O}_{v \times (N-v)} & -\mathbf{J}_v \end{bmatrix}. \end{aligned}$$

Hence, the prefix and the suffix are

$$\begin{aligned} \mathbf{x}_{pre} &= \mathbf{G}_{pre} \cdot \mathbf{x} = [x_v \quad x_{v-1} \quad \cdots \quad x_1]^T, \\ \mathbf{x}_{suf} &= \mathbf{G}_{suf} \cdot \mathbf{x} = [-x_{N-1} \quad \cdots \quad -x_{N-v}]^T. \end{aligned}$$

Hence, we have to apply a whole-point symmetry on the left and a half-point antisymmetry on the right of the original symbol. With this prefix and suffix, the channel matrix  $\mathbf{H}_{equiv}$  is perfectly diagonalized by the DCT3 odd.

### 3.3 Coefficients for the Frequency-Domain Equalizer

In this subsection all the results are valid for both DCT3 even and DCT3 odd. In both cases we have that  $\mathbf{H}_{equiv}$  is diagonalized by the corresponding DCT3 (even or odd) matrix  $\mathbf{C}_3$ :

$$\mathbf{C}_3 \cdot \mathbf{H}_{equiv} \cdot \mathbf{C}_3^{-1} = \mathbf{D},$$

where  $\mathbf{D} = \text{diag}(d_0, \dots, d_{N-1})$ . Moreover, from [8] (page 2635) and [9] (Tables VI and VII) we know that, if we define  $\tilde{\mathbf{h}}$  as the  $N$ -length vector  $\tilde{\mathbf{h}} = (h_0, h_1, \dots, h_v, 0, \dots, 0)$ , then these diagonal entries are given as follows,

- For the DCT3e:  $\mathbf{d} = \text{DCT3e}(\tilde{\mathbf{h}}) = \mathbf{C}_{3e} \cdot \tilde{\mathbf{h}}$ .
- For the DCT3o:  $\mathbf{d} = \text{DCT3o}(\tilde{\mathbf{h}}) = \mathbf{C}_{3o} \cdot \tilde{\mathbf{h}}$ .

In other words, the diagonal entries are computed as a DCT3 (even or odd, given by [9]) of the zero-padded vector  $\tilde{\mathbf{h}}$  of length  $N$ .

There is an alternative expression of  $\mathbf{d}$  analogous to the one given by Al-Dhahir for the DCT2e [4], as

$$d_i = \frac{(\mathbf{C}_3 \cdot \mathbf{H}_{equiv})_{i,0}}{c_{i,0}} = (\mathbf{C}_3 \cdot \mathbf{H}_{equiv})_{i,0} \quad (6)$$

by means of the DCT3 of the first column of  $\mathbf{H}_{equiv}$ ; but notice that this vector turns out to be equal to  $\tilde{\mathbf{h}}$ , so the expression is obviously equal to  $\mathbf{d} = \mathbf{C}_3 \cdot \tilde{\mathbf{h}}$ , as we have already claimed. Therefore, when using the DCT3, the expression (6) for the coefficients of the frequency-domain equalizers turns out to be much simpler than the one obtained in [4] for the DCT2 even.

In all cases, we can rewrite

$$\mathbf{y} = \mathbf{H} \cdot \mathbf{x}_e + \mathbf{z} = \mathbf{H}_{equiv} \cdot \mathbf{x} + \mathbf{z} = \mathbf{C}_3^{-1} \cdot \mathbf{D} \cdot \mathbf{C}_3 \cdot \mathbf{x} + \mathbf{z}$$

as

$$\mathbf{C}_3 \cdot \mathbf{y} = \mathbf{D} \cdot \mathbf{C}_3 \cdot \mathbf{x} + \mathbf{C}_3 \cdot \mathbf{z}.$$

In summary, if we denote the DCT 3 (even/odd) of  $\mathbf{x}, \mathbf{y}, \mathbf{z}$  respectively as  $\mathbf{X} = \mathbf{C}_3 \cdot \mathbf{x}$ ,  $\mathbf{Y} = \mathbf{C}_3 \cdot \mathbf{y}$  and  $\mathbf{Z} = \mathbf{C}_3 \cdot \mathbf{z}$ , then

$$\mathbf{Y} = \mathbf{D} \cdot \mathbf{X} + \mathbf{Z}.$$

Hence, the original symbol  $\mathbf{X}$  can be reconstructed from  $\mathbf{Y}$  by using 1-tap per subcarrier equalizers, given by the inverses of  $d_i$ , where  $\mathbf{d}$  is also computed by using DCT3 even/odd:

$$\mathbf{d} = \mathbf{C}_3 \cdot \tilde{\mathbf{h}}.$$

Notice that all the computations involve the DCT3, with no need of implementing other DCTs.

## 4. EXAMPLE DESIGN

Computer simulations are herein included to show the performance of the DCT3e-based MCM<sup>1</sup>. In order to achieve this goal, the bit-error rate (BER) has been evaluated in several scenarios, and compared to OFDM under the same conditions. For each simulation, 128 subcarriers are considered, two-million binary data were generated, modulated by QPSK modulation, and fed into both the proposed and the OFDM systems. It is assumed that the receiver has perfect timing synchronization and channel estimation.

Our first set of experiments considers a discrete-time memory-less Gaussian channel in Fig. 1. The BER performances (shown in Fig. 3) under additive Gaussian noise (AWGN) show that OFDM outperforms DCT3e.

The second communication scenario is that of Fig. 2. In this block of simulations, we also consider the presence of carrier frequency offset (CFO) with a value  $\Delta fT = 0.1$ . To compare the above with OFDM, we used the results presented in [10]. The resulting bit error rates obtained after the simulation are also shown in Fig. 3 and, as it can be seen, the BER of the proposed system is below  $10^{-5}$  for  $E_b/N_o \geq 19.6$  dB, whereas for OFDM the same BER value is obtained for  $E_b/N_o \geq 27.4$ .

We have studied the effects of the same CFO and a narrow-band interference signal present during the entire transmission time. The narrow-band interference is modelled as a 2nd-order Gaussian autoregressive process:

$$i_k = \sum_{n=1}^p \varphi_n \cdot i_{k-n} + e_k,$$

where  $p = 2$ ,  $\{e_k\}$  is a white Gaussian process, and the AR parameters  $\varphi_1$  and  $\varphi_2$  are assumed to be constant. In order to obtain the AR interference affecting intermediate subchannels, white Gaussian noise is passed through a second-order IIR filters with poles at  $0.92e^{\pm j\pi/3}$ . In Fig. 3 it can be seen that under narrow-band interference, the DCT3e-based MCM system shows BER values below  $10^{-5}$  for  $E_b/N_o \geq 24.7$  dB, whereas OFDM suffers from an important degradation.

In the third set of experiments, the performance of DCT3e-based system and OFDM, operating at  $E_b/N_o = 35$  dB and considering an ideal channel and the presence of CFO, is studied. The results are given in Fig. 4 and show DCT3e-MCM outperforms OFDM for  $\Delta fT < 0.14$ .

## 5. CONCLUSIONS

We have proposed DCT Type-III for MCM applications. In order to transmit each data symbol using the DCT3 even, it suffices to apply a whole-point symmetry on the left and

<sup>1</sup>The results are similar for DCT3o.

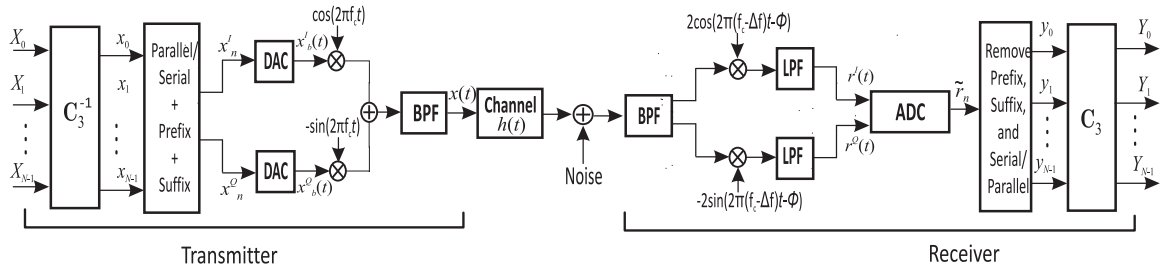


Figure 2: Block diagram of a DCT-III-based system in the presence of CFO and phase error.

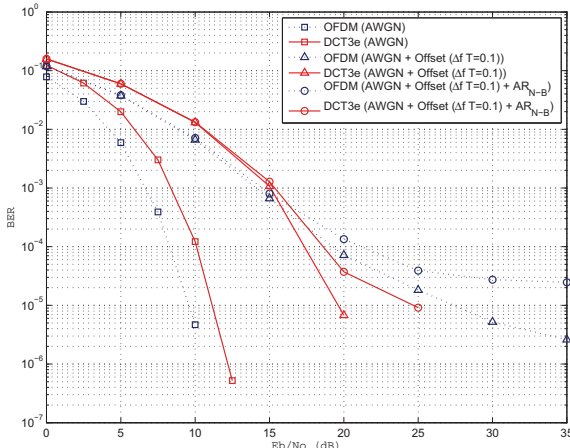


Figure 3: BER performance for DCT3e and OFDM under AWGN, CFO, and a narrow-band interference signal.

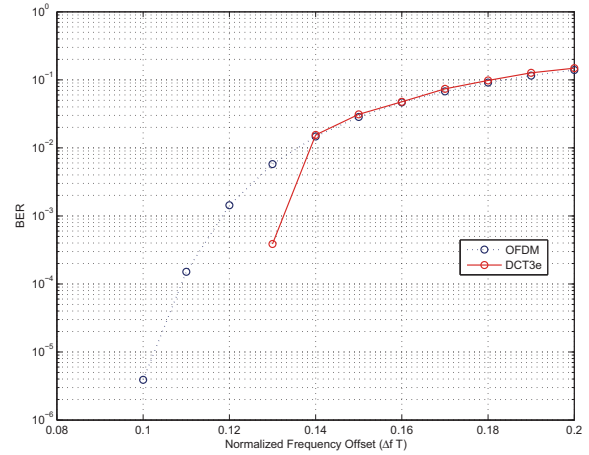


Figure 4: BER performance results for DCT3e-MCM and OFDM considering 128 subcarriers and QPSK modulation in the presence of CFO.

a whole-point antisymmetry on the right of the original symbol. On the other hand, when DCT3 odd is used, we have to apply a whole-point symmetry on the left and a half-point antisymmetry on the right of the original symbol. This prefix and suffix make the channel matrix perfectly diagonalizable by the corresponding DCT3. Hence, the coefficients of the frequency-domain equalizer are easily derived; moreover, they are also directly obtained through a DCT3. All these properties make DCT Type-III an alternative to DFT and DCT Type-II techniques. Experimental results illustrate that the proposed technique outperforms OFDM in some scenarios under CFO.

## REFERENCES

- [1] IEEE 802.11g-2003, Further Higher-Speed Physical Layer Extension in the 2.4 GHz Band, 2003.
- [2] ITU-T Recommendation G.992.5, Asymmetric digital subscriber line (ADSL) transceivers - Extended bandwidth ADSL2 (ADSL2plus), 2005.
- [3] ITU-T Recommendation G.993.2, Very high speed digital subscriber line 2 (VDSL2), 2006.
- [4] N. Al-Dhahir, H. Minn, and S. Satish, "Optimum DCT-based multicarrier transceivers for frequency-selective channels," *IEEE Trans. on Communications*, vol. 54, no. 5, pp. 911-921, May 2006.
- [5] P. Tan and N. C. Beaulieu, "A comparison of DCT-based OFDM and DFT-based OFDM in frequency offset and fading channels," *IEEE Trans. on Communications*, vol. 54, no. 11, pp. 2113-2125, Nov. 2006.
- [6] M. Elhadad, S. A. El-Dolil, and Y. A. Albagory, "Application of trigonometric transforms in discrete multi tone systems," in *Proc. of ICCES 2009*, 14-16 Dec. 2009, pp. 171-176.
- [7] A. Cero, A. Barbieri, G. Colavolpe, and M. P. Wylie-Green, "DCT-based multicarrier schemes for doubly-selective channels," in *Proc. of Waveform Diversity and Design Conf.*, 8-13 Feb 2009, pp. 307-311.
- [8] V. Sánchez, P. García, A. M. Peinado, J. C. Segura, and A. J. Rubio "Diagonalizing properties of the Discrete Cosine Transforms," *IEEE Trans. on Signal Processing*, vol. 43, no. 11, pp. 2631-2641, Nov. 1995.
- [9] S. A. Martucci, "Symmetric convolution and the Discrete Sine and Cosine Transforms," *IEEE Trans. on Signal Processing*, vol. 42, no. 5, pp. 1038-1051, May 1994.
- [10] K. Sathanathan, "Probability of error calculation of OFDM systems with frequency offset," *IEEE Trans. on Communications*, vol. 49, no. 11, pp. 1884-1888, Nov. 2001.